Published online 17 November 2015

Nucleic Acids Research, 2016, Vol. 44, No. 5 ***e48***
doi: 10.1093/nar/gkv1246

Improved knockdown from artificial microRNAs in an enhanced miR-155 backbone: a designer's guide to potent multi-target RNAi

Daniel K. Fowler[1,2], Carly Williams[2], Alida T. Gerritsen[3] and Philip Washbourne[2,*]

[1]Institute of Molecular Biology, University of Oregon, Eugene, OR 97403, USA, [2]Institute of Neuroscience, University of Oregon, Eugene, OR 97403, USA and [3]Institute for Bioinformatics and Evolutionary Studies, University of Idaho, Moscow, ID 83844, USA

Received April 22, 2015; Revised October 07, 2015; Accepted October 31, 2015

ABSTRACT

Artificial microRNA (amiRNA) sequences embedded in natural microRNA (miRNA) backbones have proven to be useful tools for RNA interference (RNAi). amiRNAs have reduced off-target and toxic effects compared to other RNAi-based methods such as short-hairpin RNAs (shRNA). amiRNAs are often less effective for knockdown, however, compared to their shRNA counterparts. We screened a large empirically-designed amiRNA set in the synthetic inhibitory BIC/miR-155 RNA (SIBR) scaffold and show common structural and sequence-specific features associated with effective amiRNAs. We then introduced exogenous motifs into the basal stem region which increase amiRNA biogenesis and knockdown potency. We call this modified backbone the enhanced SIBR (eSIBR) scaffold. Using chained amiRNAs for multi-gene knockdown, we show that concatenation of miRNAs targeting different genes is itself sufficient for increased knockdown efficacy. Further, we show that eSIBR outperforms wild-type SIBR (wtSIBR) when amiRNAs are chained. Finally, we use a lentiviral expression system in cultured neurons, where we again find that eSIBR amiRNAs are more potent for multi-target knockdown of endogenous genes. eSIBR will be a valuable tool for RNAi approaches, especially for studies where knockdown of multiple targets is desired.

INTRODUCTION

The advent of molecular techniques based on RNA interference (RNAi) has opened many avenues to researchers for genetic manipulation (reviewed in 1). RNAi is a cellular pathway which uses short interfering RNAs (siRNAs) for posttranscriptional gene regulation mainly through the biogenesis and use of microRNAs (miRNAs) (for review see 2–4). Endogenous miRNAs are hairpin-like secondary structures found in many primary RNA transcripts (pri-miRNAs). In the nucleus, the microprocessor Drosha/DGCR8 complex binds and cleaves the basal stem of pri-miRNAs to liberate the stem-loop precursor miRNA (pre-miRNA). Pre-miRNAs are then exported from the nucleus where the loop is cleaved by Dicer/TRBP to form a mature RNA duplex. The guide strand, also known as targeting strand, is separated from the passenger strand and loaded onto an argonaute protein in the RNA induced silencing complex (RISC), which then targets complementary mRNA transcripts for degradation or translational repression.

Common methods for RNAi involve the use of vector-based expression of ≈19–24 nucleotide short hairpin RNAs (shRNAs) or synthetic targeting sequences embedded in endogenous miRNA backbones (artificial miRNAs, amiRNAs). Although functional backbones for amiRNA expression have been made from a number of naturally-occurring miRNAs (5–10), the two most commonly used amiRNA scaffolds are derived from either miR-30 or the synthetic inhibitory BIC/miR-155 RNA (SIBR) (11,12), especially since commercial vectors have been developed using these backbones (Open Biosystems Expression Arrest™, GE Dharmacon and Block-iT Pol II miR RNAi™, Life Technologies, respectively). amiRNAs are embedded in sequences driven by RNA Polymerase II (Pol II) promoters, whereas shRNA expression is typically driven by constitutive Pol III promoters, such as H1 or U6. While there are conflicting reports, shRNAs generally outperform miRNAs for knockdown efficacy, likely due to higher shRNA expression levels using Pol III promoters (13–16).

Potent knockdown using shRNAs often comes at a cost, however, as at least three problems frequently arise from shRNA overexpression. First, high levels of shRNAs can cause toxicity due to oversaturation of the endogenous miRNA pathway (17–19). Oversaturation may even result in lethality during *in vivo* studies (20). amiRNAs are typ-

*To whom correspondence should be addressed. Tel: +1 541 346 4138; Fax: +1 541 346 4548; Email: pwash@uoneuro.uoregon.edu

ically expressed at much lower levels and do not saturate endogenous RNAi pathways (13,21,22). As such, amiRNAs are suitable for studies where shRNAs were toxic (23–25). Second, shRNA sequences are usually designed with perfectly-matched guide and passenger strands. In contrast, amiRNAs are often designed with central mismatches between the guide and passenger strands, which may reduce off-target effects by decreasing unwanted passenger strand incorporation into RISC (26,27). Third, shRNAs often induce an immune response which may compound or mask RNAi-specific effects (28–33). Use of amiRNAs may circumvent this problem by avoiding immune activation (23,34).

amiRNAs allow greater vector design flexibility and diversity of application compared to shRNAs. For example, amiRNAs can be co-expressed with transgenes from a single cistron driven by Poll II promoters, such as cell-specific or conditional promoters (16,24,35–37). amiRNAs can also be placed in an intron so that miRNA processing does not interfere with transgene expression (11,38). Indeed, it was originally shown that intronic SIBR amiRNAs are more potent than their exonic counterparts (11). Further, amiRNAs can easily be chained in tandem, either to increase knockdown efficiency or to target multiple genes, without the need of dedicated promoters for each hairpin sequence (9,11,39,40). Chained amiRNAs are particularly powerful tools for systems requiring multiple-target knockdown, such as studying functionally-redundant genes. For example, functional compensation often arises from gene duplications, which can mask phenotypes in single-knockout animals (41). Targeted knockdown of multiple genes can be used to overcome functional redundancy, without the need for more difficult and laborious techniques such as conditional multi-gene knockout animals. Furthermore, combinatorial amiRNA holds great promise for many gene therapies including those targeting rapidly-evolving pathogens (42,43) or human diseases caused by multiple factors, including cancer (44,45)

Currently, many researchers choose to use shRNAs based solely on the potential for greater knockdown. Because of the advantages afforded by miRNAs, enhanced knockdown rivalling that of shRNAs would be quite beneficial for many applications. Targeted optimization of miRNA scaffolds using insights gained from an improved understanding of miRNA function holds promise for increasing knockdown potency (26,46). For example, a recent deep-sequencing study uncovered conserved sequence elements of miRNA backbones that are associated with increased miRNA biogenesis and enhanced knockdown efficiency, including common UG and CNNC motifs at the basal stem region (47). Using this knowledge, an improved amiRNA backbone that enhanced microprocessor cleavage and knockdown potency, termed 'miR-E', was created by reintroduction of the wild-type CNNC motif into the commonly used miR-30 scaffold (46).

Despite enormous advancement in algorithms and rules for designing functional RNAi sequences over the last decade, the process of screening for potent sequences is often time-consuming, costly and laborious. In the present study, we suggest important criteria for effective amiRNA design. We also create and systematically test an enhanced SIBR (eSIBR) backbone containing exogenous UG and CNNC motifs at the basal stem which boosts relative amiRNA knockdown potency compared to the wild-type SIBR (wtSIBR) backbone. We find chaining amiRNAs targeting different genes is itself sufficient to enhance knockdown of each individual gene, and that eSIBR outperforms wtSIBR for multi-gene knockdown in lentiviral-transduced primary cultured hippocampal neurons. Taken together, this study presents a template for developing and expressing amiRNAs for potent multi-target RNAi.

MATERIALS AND METHODS

Expression vectors and constructs

GFP-SIBR vectors. EGFP coding sequence was inserted into HindIII and BamHI sites of pcDNA3 (Invitrogen) to make CMV-GFP. The 150 nucleotide SIBR minimal region was amplified from Ui4-SIBR-GFP (11) and inserted between the EcoRI and XbaI sites of CMV-GFP to make CMV-GFP-SIBR using primers SIBR_f and SIBR_r. Ui4-SIBR-GFP was graciously provided by Dr David Turner (University of Michigan). To allow cloning of miRNA targeting sequences into the SIBR cassette using BbsI as previously described (11), the single native BbsI site in CMV-GFP-SIBR was silently mutated by site-directed mutagenesis (Agilent). Site-directed mutagenesis was used to introduce basal UG and CNNC motifs and to generate GFP-eSIBR (Figure 3A). The G at position –15 and +14 were also changed to U in order to maintain the proper predicted folded structure. The CNNC motif was inserted beginning at position +19 due to an unusual 2 nucleotide bulge at positons +2 and +3 in the predicted folded miR-155 backbone. The inserted position of the CNNC motif is therefore equivalent to the +17 position of miRNAs without a 3′ mismatch bulge. To complete the CNNC motif, the C at position +18 was changed to U because it was shown that a C preceding the CNNC motif of miR-30 inhibited knockdown efficiency (46). The GFP-eSIBR vector has been deposited with Addgene (www.addgene.org). amiRNA sequences (Supplementary Table S1) were cloned into the SIBR cassette and chained as previously described (11). Scrambled control guide strand sequences used were scrambled1: 5′-AUUCUAAUACUACGUUCCGCAU-3′, scrambled2: 5′-ACAACUUGUAUAUCGCGCAACU-3′ and scrambled3: 5′-GAUCUUAUACUCGUGAUUGAGA-3′.

Viral vectors. The gateway cloning system (Invitrogen) was used to make viral vectors. To express miRNAs intronically, entry vector pME-SIBR was cloned by amplification of UI4-SIBR-GFP immediately following the Ubiquitin C promoter and ending shortly after the final intron/exon boundary using primers Ui4_SIBR_attBf and Ui4_SIBR_attBr, then inserted into pDONR221. The pME-SIBR vector has been deposited with Addgene. Single or triplet SIBR cassettes were shuttled to pME-SIBR from GFP-SIBR using EcoRI and XhoI. For entry vector p5E-CMV the CMV promoter sequence of pcDNA3 was cloned into pDONR221 P4-P1R using primers CMV_attBf and CMV_attBr. For entry vector p3E-nlsGFP, nlsGFP was amplified from pME-nlsGFP (48) and inserted into

pDONR221 P2R-P3 with primers nlsGFP_attBf and nlsGFP_attBr. The viral vector LV-CMV-SIBR-nlsGFP was made using the above entry vectors in an LR reaction with a Gateway-compatible third generation lentiviral destination vector kindly provided by Dr Kryn Stankunas (University of Oregon).

HA-reporter vectors. Generation of HA-Cadm1 and HA-Neuroligin1 vectors were previously described (49,50). To make HA-Cadm2 and HA-Cadm3 expression vectors, Cadm2 and Cadm3 coding regions were amplified by polymerase chain reaction (PCR) from mouse cDNA and inserted into pcDNA3 using primer pairs Cadm2_f/r for Cadm2 and Cadm3_f/r for Cadm3. HA tags were then inserted following the signal sequences with the megaprimer PCR technique using megaprimer HA-Cadm2_mp for Cadm2 and HA-Cadm3_mp for Cadm3. HA-Neuroligin2, HA-Neuroligin3, HA-Neurexin1, HA-Neurexin2 and HA-Neurexin3 vectors were kindly provided by Dr Peter Scheiffele (University of Basel, Switzerland) and have been previously described (51–53). All primer sequences are listed in Supplementary Table S2.

amiRNA design

amiRNA sequences were designed with considerations of previously described criteria for effective shRNA and miRNA sequences where possible (54–58). Briefly, specific nucleotides included a U or A (preference for U) at guide position 1 relative to the 5′ microprocessor cleavage site, U/A preferences in positions 2–7, 10–14 and 17, and G/C preferences in positions 19–21. Another prominent consideration was to design sequences with an optimal G/C content between 36.4% and 45.5% when possible. Guide strands were also designed to be 2 nucleotides longer than the passenger strand as in the original report (11). Mismatches were positioned when possible to make three general structural categories: (i) a 'loop' mismatch where 3–5 adjacent nucleotides of the guide strand were not base paired to the target strand, (ii) a '3bp-spaced' mismatch where 2 single guide strand nucleotide mismatches were separated by 3 guide/passenger base pairs and (iii) a '4bp-spaced' mismatch where 2 single guide strand nucleotide mismatches were separated by 4 guide/passenger base pairs. Of our 129 amiRNA sequences, 9 did not fold into a secondary structure fitting the above categories and 6 amiRNA sequences were designed with two alternative mismatch structures (Supplementary Table S1). For all amiRNA sequences, mismatches ranged between guide positions 11 and 17. Predicted RNA secondary structures were generated using Mfold (59). Schematics of miRNA secondary structures were drawn using VARNA (60).

Mismatch structure and sequence-specific biases

We determined the frequency (with a range of 0–1) of mismatch structures within our effective, ineffective and total amiRNA sequences. For each structural class, we calculated effective and ineffective amiRNA structure bias as the deviation of the observed frequency from the expected frequency of the total amiRNA set. Frequencies of nucleotides at specific guide strand positions were determined for our empirically-screened inefficient amiRNA sequences, and the combined efficient amiRNA set containing our screened efficient sequences and additional sequences obtained from primary literature (Supplementary Table S1). Nucleotide frequencies were calculated using custom scripts built using the ShortRead package (61) in R (R Foundation for Statistical Computing, Vienna, Austria). Nucleotide frequency biases were calculated as deviation of the observed nucleotide frequency at each position of the guide strand from an unbiased expectation of 0.25. To remove the effect of design bias, we normalized the frequency bias of the effective amiRNAs by subtracting frequency biases for the ineffective amiRNAs.

qRT-PCR

First-strand cDNAs were synthesized from total RNA isolated following COS7 cell transfections using Superscript III reverse transcriptase (Invitrogen). For experiments comparing pri-miRNA levels of target sequences in different SIBR backbones, cDNAs were created using oligodT primers for 50 min at 50°C. For experiments comparing chaining-based effects, random hexamer primers were used with synthesis at 55°C for 1 h. In both cases, pri-miRNA levels were first normalized to gapdh levels as a loading control. Rat gapdh primers were qRat_gapdh_f/r. For experiments comparing pri-miRNA levels of target sequences in different SIBR backbones the primer pair qSIBR_f/r flanking the 5′ and 3′ microprocessor cut sites in the SIBR backbones was used. For experiments comparing chaining-based effects, primer qSIBR_f was used with hairpin–specific reverse primers for cadm1.1358 (qCadm1.1358_r) and nlgn2.1283 (qNlgn2.1283_r). qRT-PCR was performed using SYBR Green reagents (Kapa Biosystems) on a StepOnePlus Real-Time PCR System (Applied Biosystems). Values and relative expression levels were compared using the $\Delta\Delta C_t$ method. Primer sequences are listed in Supplementary Table S2.

Lentiviral production and titration

2.5×10^6 HEK293T cells were plated per 10-cm tissue culture dishes in 10ml of DMEM (Invitrogen), 10% FCS, 25 units/ml penicillin & 25 μg/ml streptomycin (Sigma). ≈24 h after plating, cells were transiently transfected using calcium-phosphate with 20 μg LV-CMV-SIBR-nlsGFP vectors and packaging vectors (10 μg pMDL g/p RRE, 5 μg pRSV-Rev, 6 μg pVSV-G) (62). 6–8 h later media was replaced with 6ml/plate of fresh medium. Medium was collected 48–72 h after transfection and centrifuged at 3000xg for 5 min at RT. Supernatant was passed through a 0.45 μm syringe filter and virus was concentrated by centrifugation on a 150 000 MWCO column (Pierce). 20 000 HEK293T cells were plated per well of a 12-well plate and transduced with serial dilutions of concentrated lentivirus. 4–5 days after transduction, titres were calculated by flow cytometry on an Attune® acoustic focusing cytometer (Applied Biosystems) for GFP+ cells. Infectious lentiviral particles/μl were calculated from viral dilutions where cells were transduced in the linear range (5–20% GFP+ cells).

COS7 cell culture and transfection

COS7 cells (ATCC® Manassas, VA) were plated at a density of 50 000 cells per well of a 12-well tissue culture plate and maintained in DMEM (Invitrogen), 10% FCS, 25 units/ml penicillin & 25 μg/ml streptomycin (Sigma). ≈24 h after plating, media was replaced with DMEM, 10% FCS without pen/strep and cells were transiently transfected with Lipofectamine 2000 (Invitrogen) for ≈18 h, at which point media was replaced with DMEM, 10% FCS with pen/strep. 1 μg of reporter vector and 2 μg of GFP-SIBR vectors per well were co-transfected for knockdown experiments. For transfections for harvesting total RNA for qPCR, 1 μg of GFP-SIBR vectors were transfected per well. Cells were harvested 48–72 h following transfection.

Primary hippocampal cell culture and viral transduction

Hippocampal cultures were prepared from embryonic day 19 Sprague-Dawley rat pups as described (63), with minimal modifications. 100 000 cells were plated per well of a 12-well tissue culture plate coated with poly-L-lysine (Sigma, St. Luis, MO) in plating media (MEM (Invitrogen), 10% FCS, 20 mM dextrose, 25 units/ml penicillin and 25 μg/ml streptomycin) and incubated for 5–6 h. Media was then changed to maintenance media (Neurobasal medium (Invitrogen), 1X B-27 supplement (Invitrogen), 0.5 mM Glutamax (Invitrogen), 50 units/ml penicillin, 50 μg/ml streptomycin and 0.07% β-mercaptoethanol). Half changes of maintenance media were performed every 3–4 days in culture. 200 000 infectious viral particles, as calculated by our titration method, were added per well to transduce neurons at 2DIV. Cells were harvested at 14DIV. Studies were conducted in accordance with University of Oregon Institutional Animal Care and Use Committee protocols and in compliance with NIH guidelines for the care and use of vertebrate animals.

Quantitative western blotting

Cells were harvested after a brief wash with 1X PBS using 2X Laemmli buffer (125 mM Tris pH 6.8, 20% glycerol, 4% SDS, 0.004% bromophenol blue) with 5% beta-mercaptoethanol. Samples were heated at 95°C for 5 min, and proteins were separated by SDS-PAGE before transfer to a nitrocellulose membrane. Membranes were blocked for 1h with 3% milk in PBS and treated with primary antibodies in 3% milk/PBS overnight at 4°C. The next day membranes were washed 3 × 5 min with PBS, shaken with secondary antibody in 3% milk/PBS for 1 hr at RT, washed 3 × 5 min with PBS and imaged with an Odyssey-Fc quantitative western blot system (LI-COR). Intensities were quantified per manufacturer's instructions. Primary antibodies used were actin (mouse, 1:2000, Millipore), HA.11 (mouse, 1:2000, Covance), GFP (chicken, 1:2000, Aves Labs), Cadm1 (chicken, 1:1000, MBL International), Cadm3 (rabbit, 1:1000, Sino Biological) and Pleio-Cadm (rabbit, 1:1000, Pierce). Secondary antibodies used were anti-mouse and anti-chicken IRDye 680RD, anti-rabbit and anti-chicken IRDye 800CW (donkey, 1:1000, LI-COR). Intensities were normalized to actin loading controls. Knockdown efficiency was calculated by setting levels relative to the empty GFP-wtSIBR controls for COS7 cell experiments or uninfected (no virus) controls for neuronal cultures. Potency-of-knockdown was a metric with arbitrary units used to compare relative changes in knockdown efficacy between two conditions, and was calculated by dividing remaining reporter level (100%—knockdown efficiency) in a control condition (such as amiRNA in wtSIBR backbone or single amiRNA cassette) by the remaining reporter level in a comparison condition. Potency-of-knockdown for the control condition was set to 1.

Statistical analysis

Where noted, *P*-values obtained by statistical comparisons of two sample groups used Student's two-tailed, unpaired *t*-tests and comparisons of more than two sample groups used one-way ANOVAs followed by Tukey's post-hoc pairwise comparisons. For mismatch structure analysis, we performed Pearson's χ^2-tests ($\alpha = 0.05$) which compared observed versus expected number of effective amiRNA and ineffective amiRNAs for each mismatch class. Expected effective and ineffective amiRNA numbers for each mismatch group were calculated using frequencies of the total amiRNA set. For nucleotide frequency analysis at specific guide strand positions, we performed individual Pearson's χ^2-tests for actual counts ($\alpha = 0.01$) or normalized expectations ($\alpha = 0.001$) which compared A,U,G and C numbers at each guide strand position against an unbiased expectation of equal base frequencies. *P*-values were adjusted using Šidák correction for inflated α levels due to multiple comparisons. χ^2-tests and *t*-tests were conducted in Microsoft Excel. ANOVAs, Tukey's post-hoc analysis and Šidák corrections were performed in R.

RESULTS

Screening empirically-designed amiRNAs uncovers sequence-specific and structural features associated with efficient sequences

To screen for effective amiRNA sequences, we used a vector with the Pol II cytomegalovirus (CMV) promoter driving expression of EGFP with the original 150bp wtSIBR cassette (11) in an exon immediately following the EGFP stop codon (GFP-wtSIBR; Figure 1A and B). We tested a set of 22-nucleotide long amiRNA targeting sequences (total of 129, Supplementary Table S1) by inserting into the guide strand position of the wtSIBR backbone (Figure 1A). amiRNAs targeted a total of nine genes spanning three neuronal cell adhesion protein families. Targeted genes were cadm1–3, nlgn1–3 and nrxn1–3 which code for the proteins Cell adhesion molecule (Cadm) 1–3, Neuroligin1–3 and Neurexin1–3, respectively. As reporters for each targeted gene, we used Pol II-promoted hemagglutinin epitope-tagged constructs (HA-reporter). Using quantitative western blotting, we screened for effective amiRNA sequences co-transfecting amiRNA-expressing vectors with their counterpart HA-reporter vectors in COS7 cells (Figure 1B). Cultures co-transfected with efficient amiRNA sequences showed decreased reporter expression compared to control cultures co-transfected with a GFP-wtSIBR vector

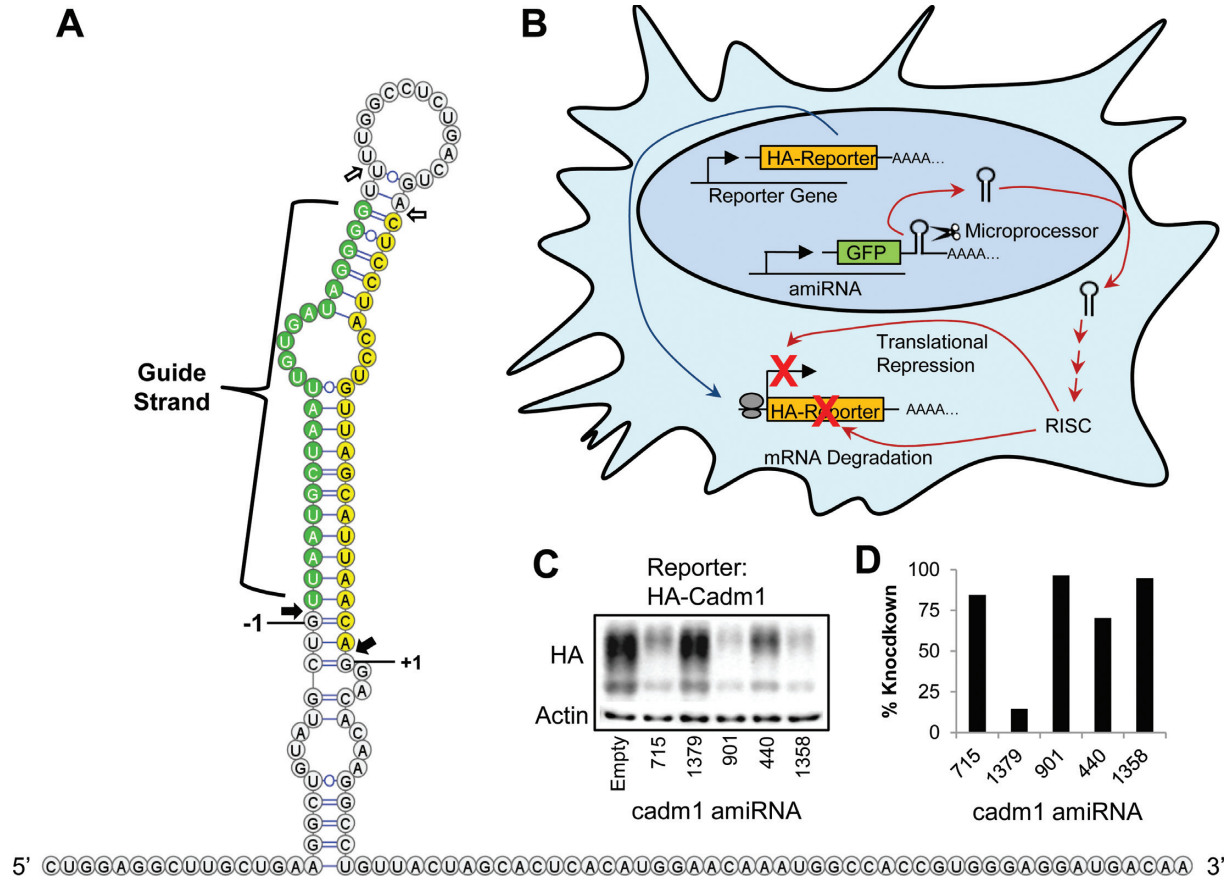

Figure 1. Overview of the wtSIBR cassette and amiRNA screening. (**A**) Nucleotide sequence of the 150-bp wtSIBR cassette from mouse and predicted miRNA secondary structure. The guide and passenger strands are labeled green and yellow, respectively. Microprocessor cleavage sites are marked with closed arrows and the +1 and –1 nucleotides relative to cleavage are indicated. Dicer cleavage sites are marked with open arrows. (**B**) Schematic representation of amiRNA screening. COS7 cells were co-transfected with an HA-tagged reporter construct and an amiRNA cloned into the guide strand position of the wtSIBR backbone located in an exon following the GFP open reading frame (GFP-SIBR). amiRNAs are liberated by the microprocessor, exported from the nucleus where they are further processed and loaded into the RNA-induced silencing complex (RISC). Effective sequences lead to reduced reporter levels due to mRNA degradation or translational repression. (**C**) Representative quantitative western blot using an HA antibody to measure reporter expression and (**D**) calculated reporter knockdown efficiency of cadm1 amiRNAs. Knockdown percentage was calculated relative to reporter co-transfection with a vector containing an empty wtSIBR cassette (empty). Actin was used as a loading control.

lacking an amiRNA targeting sequence (empty) (Figure 1C, D). Sequences which resulted in >25% reporter knockdown were considered effective and all others were considered ineffective. 50 amiRNAs were effective and 79 were ineffective for reporter knockdown (Supplementary Table S1).

Because SIBR-based amiRNAs are frequently designed with guide/passenger strand mismatches (11), we wanted to determine if mismatch structure was associated with knockdown efficiency. We grouped amiRNAs into three general categories that mimicked predicted naturally-occurring miR-155 secondary structures (Figure 2A). We found that effective hairpins were less likely to contain a loop mismatch whereas ineffective hairpins were more likely to contain a loop mismatch (Figure 2B). We also noted that effective hairpins tended to contain the 3bp-spaced mismatch structure ($P = 0.07$, Pearson's χ^2-test) and had little bias for or against the 4bp-spaced mismatch structure. The observed tendency for successful amiRNAs to contain the human mismatch structure may indicate a species-specific preference, because COS7 cells are a primate-derived line (African green monkey). Furthermore, G/C content of effective versus ineffective amiRNA sequences were compared and we found the G/C content of effective hairpins to be significantly less than ineffective hairpins (effective = 40.1% G/C, ineffective = 43.5% G/C) (Figure 2C).

Next, we examined the primary sequence factors that influenced knockdown efficiency. To do so, we mined primary literature to obtain an additional 133 effective SIBR amiRNA sequences to increase our comparison power. We then calculated the nucleotide frequency bias at individual guide strand positions for the combined effective amiRNA set ($n = 183$) and our ineffective amiRNAs ($n = 79$) (Figure 2D). Note that we did not compare position 22 because many of the hairpins we obtained from the literature were cloned into a specific miR-155 backbone (pcDNA^{TM}6.2-GW/EmGFP-miR) where position 22 is always a G. As most amiRNAs are designed using common algorithms and guidelines, it was not surprising to find significant enrichments ($\alpha = 0.01$) of either U, A or both at position 1, 2, 4, 7, 10, 12 and 14 in effective amiRNA sequences. We did note unexpected enrichment of G at position 8 and C at position 9. Also as expected, both the effective and inef-

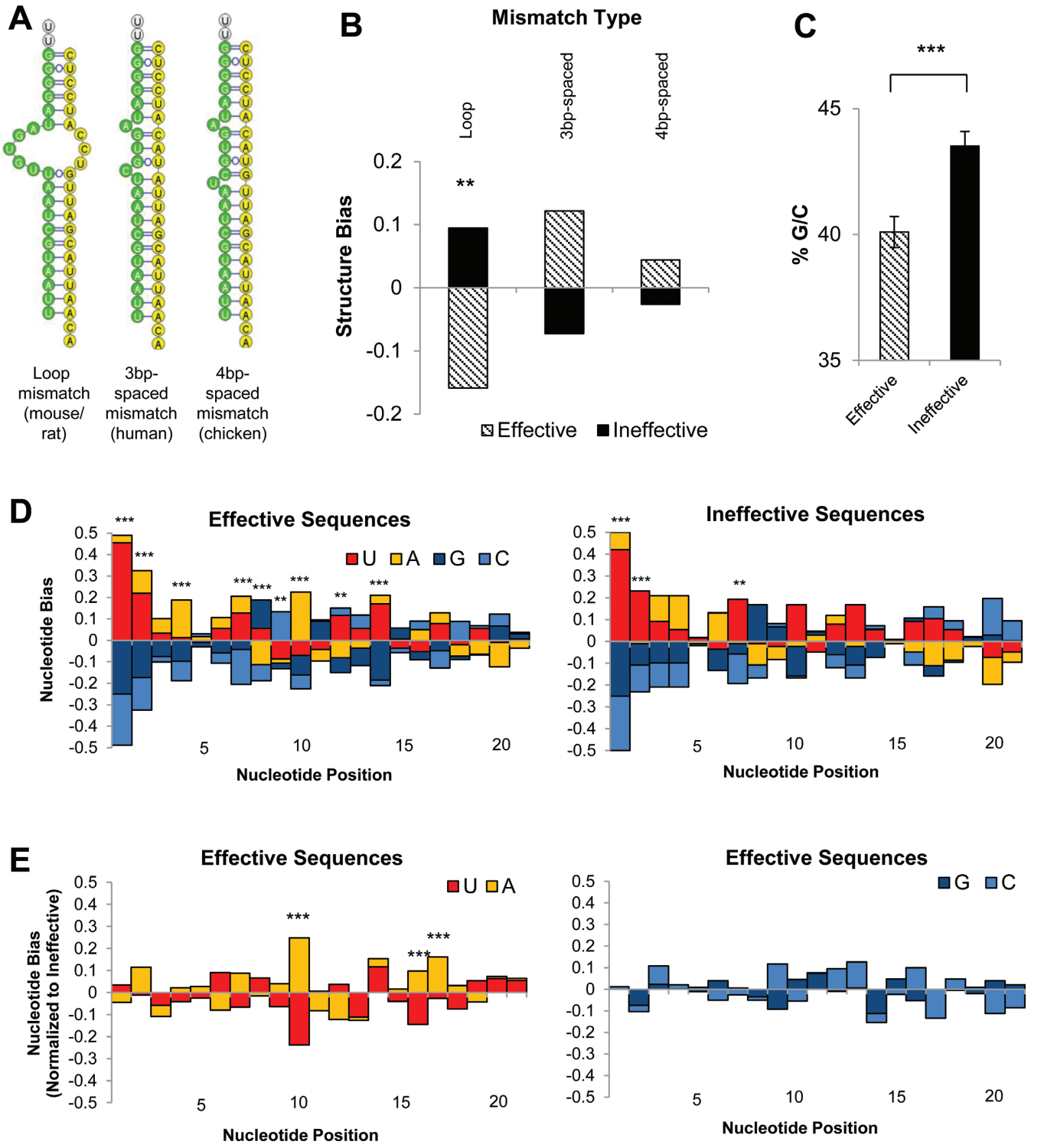

Figure 2. Distinct structural features are associated with effective and ineffective amiRNA sequences. (**A**) Example miR-155 nucleotide sequences from different organisms and predicted secondary structures of distinct guide/passenger strand mismatches. (**B**) Frequency bias of different mismatch structures found in effective and ineffective amiRNA sequences. Effective amiRNA $n = 50$, ineffective amiRNA $n = 84$, $^{**}P < 0.01$, Pearson's χ^2-test. (**C**) G/C nucleotide content of effective and ineffective amiRNA sequences. Effective amiRNA $n = 50$, ineffective amiRNA $n = 79$, $^{***}P < 0.001$ Student's two-tailed *t*-test. Error bars represent SEM. (**D**) Nucleotide frequency bias of effective and ineffective amiRNA sequences and (**E**) Normalized U/A or G/C nucleotide frequency bias of effective amiRNA sequences. Nucleotide positions are relative to the 5′ microprocessor cleavage site. Effective amiRNA $n = 183$, ineffective amiRNA $n = 79$, $^{**}P < 0.01$, $^{***}P < 0.001$ Pearson's χ^2-test with Šidák correction for multiple comparisons.

fective sequences displayed a G/C content asymmetry, with A/U-rich 5′ and G/C-rich 3′ ends. This asymmetry has been shown to influence guide strand selection, is strongly associated with effective target sequences, and is a major criteria for effective siRNA design (64,65). Additionally, nucleotide frequencies at specific positions were quite similar in effective and ineffective sequences, likely indicating design bias for both sets. To eliminate design bias, we normalized the effective sequence nucleotide frequency by subtracting the values of the ineffective data set. Because our ineffective amiRNA set was smaller than the combined effective amiRNA set, we made our analysis more stringent ($\alpha = 0.001$). Normalization removed all of the enrichments noted above except for position 10, where, strikingly, effective amiRNA sequences were likely to contain an A but not a U (Figure 2E). We did note a significant, but smaller, enrichment of A and depletion of U at positions 16 and 17. We did not find any significant bias for G or C at any position (Figure 2E). Taken together, these results highlight important criteria for designing effective amiRNA sequences.

Introduction of UG and CNNC motifs creates an enhanced SIBR (eSIBR) backbone

Because recent studies have shown that targeted adjustments to the miR-30 backbone can increase knockdown efficiency (26,46), we tested whether modifications to the wtSIBR backbone could also increase amiRNA knockdown potency. Auyeung *et al.* established that two key sequences at the basal stem in human miRNAs, the UG motif at positions –14 and –13 relative to the 5′ microprocessor cleavage site and the CNNC motif beginning between positions +16 and +18 relative to the 3′ microprocessor cleavage site, are associated with efficient miRNA processing and target knockdown (47). Neither of these motifs are present in the wtSIBR backbone, so we introduced the motifs singly or in combination to GFP-wtSIBR to create modified GFP-SIBR scaffolds (Figure 3A).

We evaluated the effect of modified SIBR backbones on amiRNA knockdown efficiency for 16 of our effective amiRNA sequences (Figure 3B–D and Supplementary Figure S1). The majority of these amiRNA sequences induced robust knockdown when expressed from the wtSIBR backbone (Figure 3C and D). In order to be confident that our quantitative Western blot assay was suitable to measure further knockdown enhancement, we tested the precision of the assay for measuring small differences in protein levels. We found that our assay was able to reliably and accurately measure differences as low as 10% of HA-reporter protein levels (Supplementary Figure S2). These results demonstrate that our quantitative Western blot assay is well suited to monitor differences in knockdown efficiencies due to backbone modifications.

We performed 3–4 replicate experiments comparing knockdown efficiencies for five of our potent (>70% knockdown) amiRNA sequences expressed from the wtSIBR or modified backbones (Figure 3B and C, Supplementary Figure S1). Changes in knockdown efficacy in response to introduction of single UG or CNNC motifs varied considerably for individual amiRNA sequences (Figure 3C). In contrast, introduction of both UG and CNNC motifs into the SIBR backbone enhanced reporter knockdown for all 16 amiRNA sequences tested (Figure 3C and D). We named this backbone containing both motifs the enhanced SIBR (eSIBR) scaffold. Because the range of reporter knockdown from amiRNAs in the wtSIBR backbone was large (≈25% to >90%; Figure 3C and D) and were difficult to compare directly, we used a relative metric that is independent of absolute knockdown percentage. This metric, which we call potency-of-knockdown, is the inverse of the amount of the remaining reporter level compared to a control condition; an amiRNA that reduced the remaining protein to 1/2 of the control amount had a 2-fold potency-of-knockdown, one that reduced remaining reporter to 1/3 had a 3-fold potency-of-knockdown. We used this metric to compare knockdown efficacy of amiRNA sequences in modified backbones relative to corresponding wtSIBR amiRNAs. The eSIBR backbone reproducibly boosted potency-of-knockdown an average of ≈2-fold over counterpart sequences in the wtSIBR backbone (Figure 3E).

The eSIBR backbone enhances cleavage by the microprocessor

To examine whether improved knockdown from the eSIBR backbone may be due to an increase in miRNA biogenesis, we used a previously established method for monitoring microprocessor cleavage (46). Because the amiRNA sequence is located in an exon following the GFP coding region, cleavage of the hairpin by the microprocessor separates the coding region from the polyA tail, which prevents nuclear export and destabilizes the mRNA, resulting in lowered GFP translation (Figure 4A). Thus, lowered GFP levels indicate enhanced microprocessor cleavage.

We used quantitative western blotting to measure GFP levels in COS7 cells transfected with GFP-SIBR vectors containing amiRNAs in the wtSIBR or modified SIBR backbones (Figure 4B). We compared GFP levels in cells transfected with amiRNAs in modified SIBR backbones relative to their wtSIBR counterparts and found decreased GFP levels in cultures expressing eSIBR amiRNAs, but not in cultures with amiRNAs in backbones containing individual UG or CNNC motifs (Figure 4C). This observation suggests that increased knockdown gained from the eSIBR backbone stems from enhanced microprocessor cleavage.

To directly monitor amiRNA processing, we performed quantitative real-time PCR (qRT-PCR) to measure unprocessed pri-miRNA levels in COS7 cells transfected with GFP-SIBR vectors and compared relative pri-miRNA levels of amiRNAs expressed from the modified SIBR backbones to pri-miRNA levels of their counterparts in the wtSIBR backbone. Mirroring the results obtained by monitoring relative GFP levels, only amiRNAs expressed from the eSIBR backbone, and not backbones with a single motif, showed significantly reduced pri-miRNA levels of ≈30% (Figure 4D and E). Because these were overexpression experiments, the observed ≈30% reduction in pri-miRNA levels due to the eSIBR modifications is not representative of single-copy kinetics and likely under-represents the increase in the amount of pre-miRNAs able to enter the RNAi pathway. Together, these results provide strong evidence that the

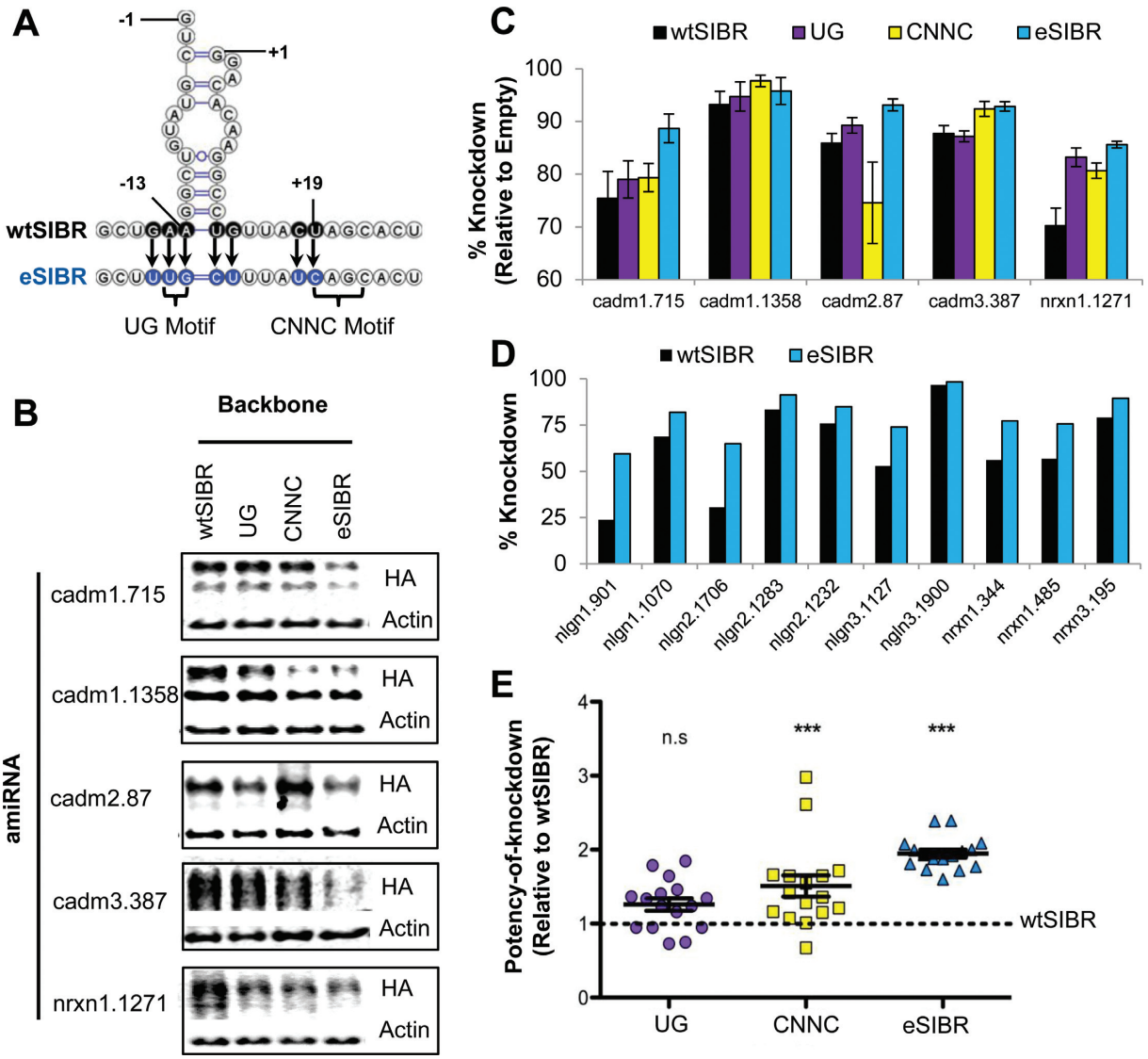

Figure 3. The eSIBR backbone enhances knockdown potency. (**A**) Nucleotide substitutions on and near the miR-155 basal stem which added the indicated UG and CNNC motifs to create the eSIBR backbone. Black circles indicate the wild-type sequence; blue circles are the modified sequence. Nucleotide numbers are relative to microprocessor cleavage sites. (**B**) Representative western blots and (**C**) quantification of reporter knockdown efficiency from data in Supplementary Figure S1 in COS7 cells co-transfected with the indicated amiRNAs in wild-type or modified SIBR backbones. Knockdown percentage was calculated relative to reporter co-transfections with a control vector containing an empty wtSIBR cassette (empty, not shown). Actin was used as a loading control. cadm1.715 and nrxn1.1271 $n = 4$ independent experiments, all others $n = 3$ independent experiments. (**D**) Reporter knockdown efficiency as in (C) from single experiments with additional amiRNAs in the wtSIBR or eSIBR backbone. (**E**) Comparison of potency-of-knockdown between constructs containing amiRNAs in modified backbones (plotted points) relative to their counterparts in the wtSIBR backbone (dotted line). If more than one experiment was conducted for an amiRNA, the average value is plotted. $n = 16$ amiRNAs, $^{***}P < 0.001$, n.s. = not significant, one-way ANOVA with Tukey's post-hoc comparison to the wtSIBR backbone group. For all graphs error bars represent SEM.

eSIBR backbone enhances knockdown through increased microprocessor cleavage and liberation of pre-miRNA hairpins.

Chaining amiRNAs targeting different genes increases knockdown potency

One useful feature of the SIBR cassette is the ability to easily chain amiRNAs in tandem (11). To simultaneously knockdown multiple genes, we chained together amiRNA triplets in the wtSIBR or eSIBR backbones, targeting three different cadm family or nlgn family genes (e.g. cadm1, 2 and 3 or nlgn1, 2 and 3) (Figure 5A). Three unique scrambled amiRNA sequences targeting no known genes served as a control (scrambled1, 2 and 3).

We wanted to determine if chaining amiRNAs in tandem influenced their individual efficacies. Because DNA sequences can be highly homologous between gene family members, we investigated potential cross-targeting of amiRNA sequences within their gene family. We monitored knockdown of HA-reporters when co-transfected with single amiRNAs against each of the family members (Figure 5B). We found that only one amiRNA, nlgn2.1283, not only reduced HA-Neuroligin2 levels but also HA-Neuroligin3

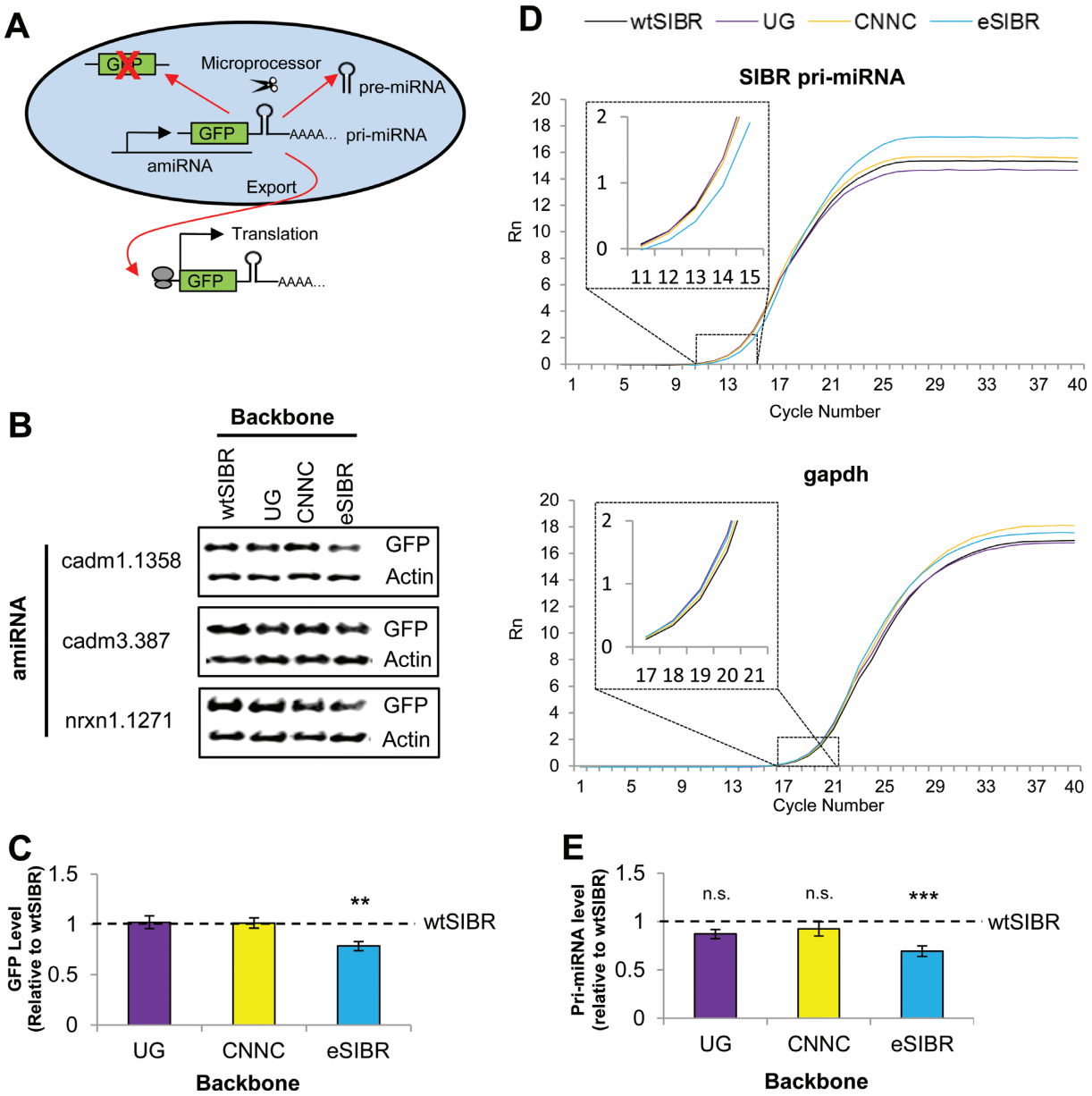

Figure 4. The eSIBR backbone increases cleavage by the microprocessor. (**A**) Schematic of microprocessor activity assay. GFP-SIBR mRNA is either exported from the nucleus to be translated or the amiRNA is cleaved by the microprocessor and the mRNA is degraded. (**B**) Representative western blots showing GFP levels in COS7 cells transfected with GFP-SIBR constructs containing the indicated amiRNAs in wild-type or modified SIBR backbones. Actin was used as a loading control. (**C**) Comparison of GFP levels measured by quantitative western blot of COS7 cells transfected with GFP-SIBR constructs carrying amiRNAs in modified backbones (bars) relative to their corresponding wtSIBR counterparts (dotted line). (**D**) Representative SIBR pri-miRNA and gapdh loading control qRT-PCR amplification plots using cDNAs synthesized from COS7 cell total RNA following transfection of hairpin nlgn3.1900 in wtSIBR or modified backbones. Insets are of the threshold cycle region of the amplification curves. (**E**) Comparison of SIBR pri-miRNA levels measured by qRT-PCR of COS7 cells transfected with GFP-SIBR constructs carrying amiRNAs in modified backbones (bars) relative to their corresponding wtSIBR counterparts (dotted line). If more than one experiment was conducted for an amiRNA sequence, the average value was used. (C) $n = 16$ amiRNAs, (E) $n = 18$ amiRNAs, $^{**}P < 0.01$, $^{***}P < 0.001$, n.s. = not significant, one-way ANOVA with Tukey's post-hoc comparison to the wtSIBR group. Error bars represent SEM.

levels, presumably due to 19/22 nucleotide homology with the target sequence. We therefore omitted HA-Neuroligin3 from subsequent analysis of linkage-based effects.

To test if multimerizing amiRNAs could alter their efficiency, we used quantitative western blotting to monitor reporter knockdown in COS7 cells co-transfected with triplet amiRNAs and their corresponding HA-reporter vectors (Figure 5C). Knockdown efficiency was measured by normalizing reporter levels to control cultures co-transfected with an empty GFP-wtSIBR vector. Again in all cases, we found that single amiRNAs in the eSIBR backbone enhanced knockdown efficiency compared to single amiRNAs in the wtSIBR backbone and increased potency-of-knockdown ≈2-fold (data not shown). Surprisingly, we

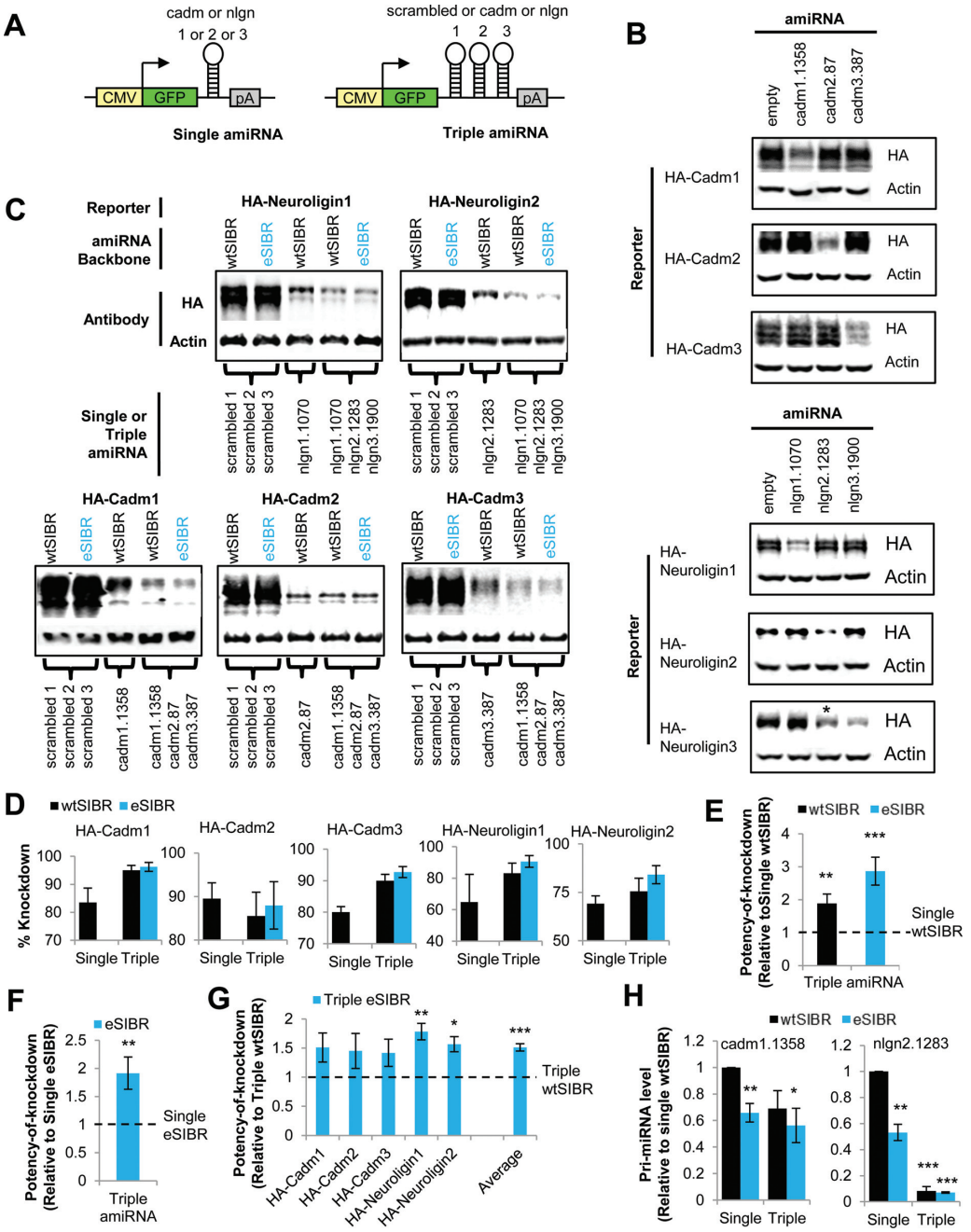

Figure 5. Chaining amiRNAs targeting distinct genes increases knockdown potency. (**A**) Schematic of GFP-SIBR constructs expressing a single hairpin or triple hairpins used in this figure. Single hairpin constructs contain an amiRNA targeting a single gene. Triple hairpin constructs contain three unique amiRNA sequences targeting different genes of the same family (e.g. cadm1, 2 and 3 or nlgn1, 2 and 3) or contain three unique scrambled sequences (scrambled1, 2 and 3). (**B**) Representative western blots showing knockdown fidelity for all combinations of HA-reporter constructs co-transfected with single wtSIBR amiRNAs and a control vector containing an empty wtSIBR cassette (empty) in COS7 cells. Cross-targeting is marked by an asterisk. (**C**) Representative western blots and (**D**) quantification of reporter knockdown efficiency in COS7 cells co-transfected with GFP-SIBR constructs carrying indicated single or triple amiRNA sequences in either wtSIBR or eSIBR backbones. Knockdown percentage was calculated relative to reporter co-transfections with a control vector containing an empty wtSIBR cassette (not shown). Data for single eSIBR amiRNAs are not shown. Actin was used as a loading control. Values represent the average of 3 independent experiments. (**E**) Comparison of potency-of-knockdown for triple-amiRNA expressing constructs (bars) relative to their counterparts with single-amiRNAs in the wtSIBR backbone (dotted line) and (**F**) comparison of potency-of-knockdown for triple eSIBR amiRNA expressing constructs (bar) relative to counterparts single amiRNAs in the eSIBR backbone from experiments in (D). Values represent the average of all values for 3 independent experiments of the 5 conditions as in (D) (total $n = 18$ per group). $^{**}P < 0.01$, $^{***}P < 0.001$, student's two-tailed t-tests against the relative control group (dotted line). (**G**) Comparison of potency-of-knockdown for triple-amiRNA constructs in eSIBR backbones (blue bars) relative to their counterparts expressing triple-amiRNAs in the wtSIBR backbone (black bars) from data in (D). $n = 3$ independent experiments, $^{*}P < 0.05$, $^{**}P < 0.01$, $^{***}P < 0.001$, Student's two-tailed t-test. (**H**) Comparison of pri-miRNA levels measured by qRT-PCR in COS7 cells following transfection of single and triple cadm1.1358- and nlgn2.1283-containing SIBR constructs in either the wtSIBR or eSIBR backbones. pri-miRNA levels are relative to the single wtSIBR amiRNA condition. $n = 3$ independent experiments, $^{*}P < 0.05$, $^{**}P < 0.01$, $^{***}P < 0.001$, Student's two-tailed t-test against the single wtSIBR amiRNA condition. For all graphs, error bars represent SEM.

found that concatenation of amiRNAs in the wtSIBR backbone targeting different genes was itself sufficient to increase knockdown efficiency for 4 of the 5 reporter constructs (Figure 5D). To compare relative effects of chaining amiRNAs across different amiRNA sequences, we calculated potency-of-knockdown for amiRNA triplets in the wtSIBR backbone compared to their corresponding single wtSIBR amiRNAs. We found that chaining wtSIBR amiRNAs significantly increased potency-of-knockdown nearly 2-fold (≈1.9-fold; Figure 5E). When compared to their single eSIBR amiRNA counterparts, triple eSIBR amiRNAs also increased potency-of-knockdown ≈1.9-fold (Figure 5F), which suggests that the eSIBR backbone modifications do not interfere with chaining-based knockdown enhancement. As each amiRNA targeted distinct genes and enhanced knockdown was still observed, our results suggest a cooperative effect for miRNA biogenesis when amiRNAs are chained in close proximity.

The eSIBR backbone enhances multi-gene knockdown

To test if eSIBR amiRNAs retain their enhanced knockdown potential when concatenated, we calculated potency-of-knockdown for triplet GFP-SIBR constructs containing amiRNAs in the eSIBR backbone relative to corresponding single or triple amiRNAs in the wtSIBR backbone. When compared to their triplet wtSIBR counterparts, triplet eSIBR amiRNAs increased potency-of-knockdown in all 5 conditions, with an average enhancement of ≈1.5-fold (Figure 5G), which is less than the expected 2-fold increase seen in single amiRNAs. When directly compared to their single amiRNA counterparts in the wtSIBR backbone, triplet eSIBR amiRNAs showed a nearly 3-fold increase in potency-of-knockdown (≈2.9-fold; Figure 5E), which is less than the expected ≈4-fold enhancement in potency-of-knockdown if both the enhancement from the eSIBR backbone and the linkage-based increase were independently additive. These two observations suggest that knockdown enhancement afforded by the eSIBR modifications is reduced when amiRNAs are multimerized. Nevertheless, these results show that chaining eSIBR amiRNAs, even when targeting distinct genes, can further boost overall knockdown potency.

Chaining-based knockdown enhancement is due to increased pri-miRNA processing

We tested if the linkage-based increase in knockdown potency due to chaining amiRNAs in tandem was also due to enhancement in microprocessor cleavage of the pri-miRNA hairpin. In order to directly compare pri-miRNA processing between single and chained amiRNAs, we designed primers to monitor the 5′-most hairpin for both the cadm1–3 and nlgn1–3 triple constructs (cadm1.1358 and nlgn2.1283, respectively) and used qRT-PCR to measure pri-miRNA levels in COS7 cells transfected with triple amiRNAs in the wtSIBR or eSIBR backbones as well as the corresponding single amiRNAs in the wtSIBR or eSIBR backbones. We again observed a significant increase in pri-miRNA processing from single eSIBR amiRNAs compared to their wtSIBR counterparts (Figure 5H). Chaining amiRNAs decreased pri-miRNA levels for both amiRNAs, although levels were reduced much more for nlgn2.1283 than for cadm1.1358 (92% and 30% reduction, respectively; Figure 5H). For both amiRNAs, triple eSIBR constructs showed a further, but more modest decrease in pri-miRNA levels compared to triple wtSIBR counterparts (Figure 5H). These results imply that knockdown enhancement due to chaining amiRNAs is from increased microprocessor cleavage.

eSIBR boosts endogenous multi-gene knockdown potency

Next, we tested the applicability of eSIBR amiRNAs for multi-gene knockdown of endogenous proteins. We generated a lentiviral vector carrying triplet amiRNAs in the wtSIBR or eSIBR backbones which target cadm1, 2 and 3. amiRNA expression is driven by the CMV promoter and located in an intron preceding the coding region for nuclear-localized GFP (nlsGFP) (Figure 6A). We placed amiRNAs in an intron because intronic expression of amiRNAs enhances target knockdown (11). We transduced cultures of rat hippocampal neurons two days after plating (days *in vitro*, DIV) with high-titre lentivirus carrying triplet cadm amiRNAs or control triplet scrambled amiRNAs. We then used quantitative western blotting to monitor endogenous Cadm protein knockdown in 14DIV cultures (Figure 6B). We measured protein levels with antibodies against endogenous Cadm1, Cadm3 or pleio-Cadm, which recognizes Cadms 1, 2 and 3 (66), and measured knockdown efficiency by normalizing values to non-infected sister cultures (no virus) (Figure 6C). For all antibodies tested, amiRNAs in the eSIBR backbone significantly enhanced knockdown efficiency (Figure 6C). We calculated potency-of-knockdown between triplet wtSIBR and eSIBR amiRNAs, and we found that the eSIBR backbone increased potency-of-knockdown an average ≈2-fold over wtSIBR amiRNAs (Figure 6D). These results show that eSIBR is more efficient than currently-used SIBR-based vectors for endogenous multi-gene knockdown.

DISCUSSION

The use of amiRNAs have been shown throughout a diverse range of experimental contexts as an efficient means for RNAi. Despite the enormous benefits associated with amiRNAs, experimental application often suffers from insufficient target knockdown compared to other RNAi-based methods. We showed here that targeted optimization of the amiRNA SIBR backbone, termed the eSIBR scaffold, greatly enhanced the relative knockdown potency of all amiRNA sequences tested. This potent effect was due to an increase in microprocessor cleavage. When we chained eSIBR amiRNAs, even when each amiRNA targeted a unique gene, potency-of-knockdown was often enhanced more than 3-fold compared to single wtSIBR amiRNAs. Therefore, the eSIBR backbone offers great potential to boost amiRNA knockdown efficacy to comparable levels with methods such as shRNA without caveats routinely encountered with other RNAi-based techniques.

Using a large empirically-designed set of amiRNAs, we found specific sequences associated with efficient amiRNA sequences. We observed that effective sequences are highly

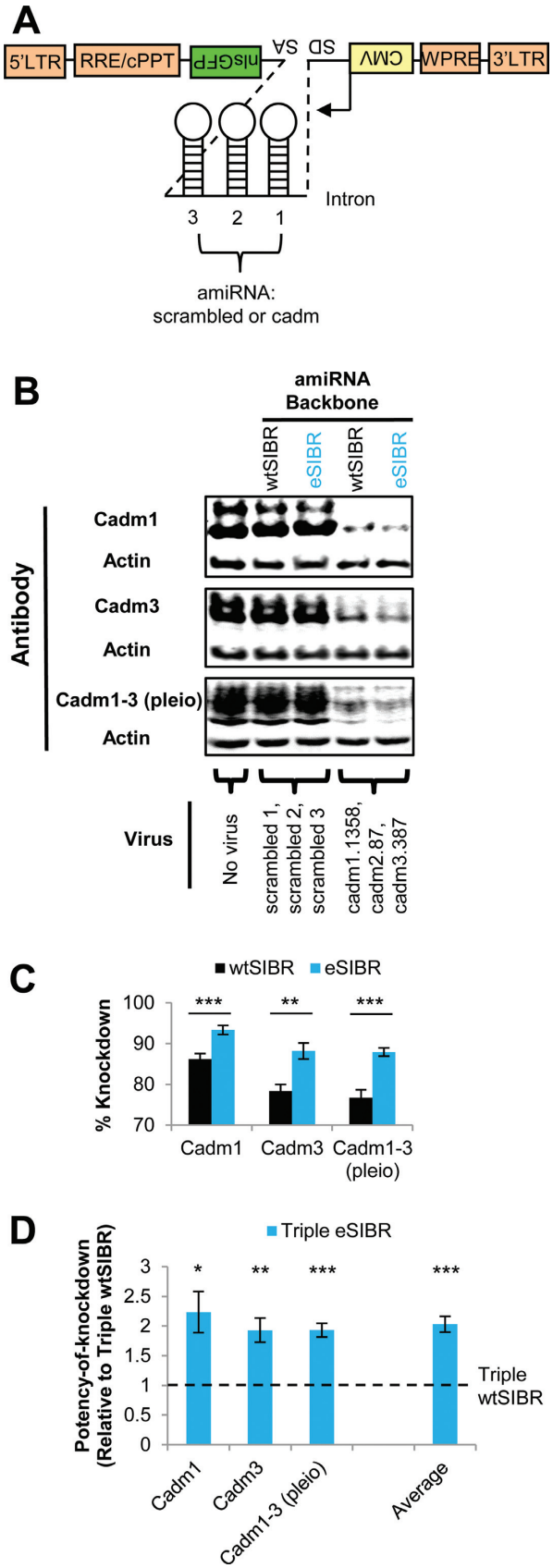

Figure 6. eSIBR enhances multi-target knockdown potency in primary neuron cultures. (**A**) Schematic of lentiviral vectors used for multiple endogenous gene knockdown. The cytomegalovirus promoter (CMV, yellow) promotes antisense-strand expression (relative to viral RNA) of amiRNAs located in an intron preceding a nuclear-localized GFP (nlsGFP, green) coding sequence. amiRNA triplets target cadm1, 2 and 3 or contain three unique scrambled sequences (scrambled1, 2 and 3). Orange boxes represent viral-specific sequences. LTR, long-terminal repeat, RRE, Rev-response element, cPPT, central polypurine tract, WPRE, woodchuck hepatitis virus posttranscriptional regulatory element, SA, splice acceptor, SD, splice donor. (**B**) Representative western blots and (**C**) quantification of endogenous Cadm family knockdown efficiency in 14DIV cultured rat hippocampal neurons transduced with viral constructs carrying the indicated amiRNA sequences in wtSIBR or eSIBR backbones. Antibodies were against Cadm1, Cadm3 or Cadm1–3 (pleio-Cadm). Knockdown percentage was calculated relative to uninfected control cultures (no virus). Actin was used as a loading control. (**D**) Comparison of endogenous Cadm potency-of-knockdown for viral vectors containing amiRNAs in eSIBR backbones (blue bars) relative to their counterparts in the wtSIBR backbone (black bars). (C) and (D) $n = 4$ independent experiments, $^{*}P < 0.05$, $^{**}P < 0.01$, $^{***}P < 0.001$, Student's two-tailed t-test. Error bars represent SEM.

biased for an A but against a U at guide position 10. Enrichment of A at position 10 has been previously noted for efficient shRNA and miR-30-based amiRNA sequences (55,57,67,68). Argonaute proteins in RISC cleave target mRNA between nucleotides complementary to guide strand positions 10 and 11. Bias for A at guide position 10 in effective sequences may arise from increased mRNA cleavage efficiency because a U in the mRNA complementary to guide position 10 is the preferred substrate (57). However, most previous studies also noted an enrichment of U at position 10 as well (57,67,68). In particular, studies which screened for effective amiRNA sequences using the miR-30 backbone found enrichment for both A and U at position 10 (55,69), suggesting that a bias against U at position 10 may be specific for SIBR amiRNAs. Taken together, these conflicting observations posit that differences between amiRNA expression systems, such as the loop sequence or inclusion of central mismatches, may alter primary sequences important for RNAi efficacy. Thus, our results highlight the need for more context-dependent criteria for amiRNA design.

We also observed structural criteria associated with effective amiRNAs. We and others have found that G/C content of <50% is associated with effective sequences (57,70). Specifically, our experimental average of ≈40% G/C for effective amiRNAs fell precisely at the median G/C range of effective sequences in a recent, high-throughput amiRNA screen (55). We also investigated the effect of guide/passenger mismatch structure on amiRNA efficiency. We found that effective hairpins were not likely to contain an open loop mismatch and favored two mismatches separated by 3-basepaired nucleotides. We note that because COS7 cells are a monkey-derived line, the observed preference for the human mismatch structure may be due to specificities in miRNA processing machinery between species. Whether mismatch structure preference is different for SIBR-based amiRNAs in different organisms will require further investigation. Nonetheless, one should consider empirically optimizing mismatch structure when designing amiRNAs for this system if using different species. Previous studies have seen that introduction of central mis-

matches between the guide and passenger strands can improve knockdown efficacy in certain sequences (27,71), but to our knowledge this is the first report to systematically test preferred guide/passenger mismatch structures for an amiRNA system. Central mismatches can influence guide strand selection (72–74) as well as alter loading onto functionally-distinct Ago proteins in RISC. For example, siRNAs containing central mismatches shifts loading of guide strands from Ago2 to Ago1 in Drosophila, which alters target knockdown efficiency (75–77).

Thus, in addition to general considerations for effective RNAi design, our results suggest two important criteria for the design of effective SIBR-based amiRNAs: (i) inclusion of A and exclusion of U at guide position 10, and (ii) optimization of guide/passenger mismatch structure.

One interesting trend that we noticed when comparing modified backbones containing either single UG and CNNC motifs and the eSIBR backbone, which contains both, is that while both motifs generally enhanced knockdown efficiency, the effect of single motifs on the potency of individual amiRNA sequences varied considerably. In stark contrast, combining both motifs in the eSIBR backbone reproducibly enhanced potency-of-knockdown for all 16 amiRNA sequences ≈2-fold over identical sequences in the wtSIBR backbone. Because the eSIBR backbone caused such a reproducible increase in knockdown efficacy, but the effect of the individual motifs did not appear to be additive, suggests the UG and CNNC motifs are functionally linked. Indeed, we only observed increased cleavage by the microprocessor when both motifs were combined, as monitored either indirectly by GFP expression or directly by assaying pri-miRNA levels. Enhanced knockdown in the miR-30-based 'miR-E' backbone by Fellmann *et al.*, which was created by reintroducing the wild-type CNNC motif, may support this notion because miR-30 already contained the basal UG motif (46). The CNNC motif was originally shown to bind the splicing factor SRp20, and more recently the DEAD-box protein DDX17, both of which associate with and can regulate microprocessor activity, although specific modes of action are not known (47,78,79). Further work will need to determine whether these regulatory mechanisms also involve the UG motif.

Our work strongly supports increased pri-miRNA processing as the causative factor of enhanced knockdown afforded by both amiRNA chaining and the eSIBR backbone modifications. Both chaining and the eSIBR backbone decreased pri-miRNA levels, as monitored by qRT-PCR. Because an ≈2-fold increase in potency-of-knockdown was observed from both the eSIBR backbone and amiRNA chaining, we would expect an ≈4-fold enhancement to potency-of-knockdown if both factors contributed independently to knockdown efficiency. However, we observed an ≈3-fold increase when eSIBR amiRNAs were multimerized. Although more work is needed to determine molecular mechanisms responsible for this observation, it is possible that pri-miRNA processing efficiency hits a maximum level which is less than the maximum contribution from both the eSIBR backbone and linkage-based effect. Indeed, we found that the combination of both factors caused only a modest further increase in pri-miRNA processing as compared to much larger individual contributions from chaining or the eSIBR backbone alone. In further support of this notion, we determined that the lower than expected knockdown enhancement was not simply due to the eSIBR backbone interfering with the chaining effect; wtSIBR and eSIBR backbones similarly enhanced knockdown potency when multimerized. Interestingly, effects on processing efficiency may be cell or species-dependent, because we observed an expected ≈2-fold increase in potency-of-knockdown when comparing triple eSIBR amiRNAs to triple wtSIBR amiRNAs in cultured rat hippocampal neurons, but only observed a 1.5-fold enhancement in our COS7 cell assays.

Our results may also suggest that the eSIBR modifications or amiRNA chaining alter pri-miRNA processing kinetics. For example, the observed non-additive increase to knockdown potency from the combination of amiRNA chaining and the eSIBR backbone could be due to a reduction in pri-miRNA processing speed for eSIBR amiRNAs, but not wtSIBR amiRNAs, when concatenated. Moreover, the idea of different processing speeds could explain why 1 out of 5 amiRNAs tested (cadm2.87) did not exhibit a chaining-based enhancement of knockdown potency. For instance, it is possible that the cadm2.87 hairpin had a higher basal processing rate than the other amiRNAs which was not further increased by amiRNA chaining. More work is needed to investigate the exact influence of amiRNA concatenation and the eSIBR backbone on miRNA processing kinetics.

We believe that the eSIBR backbone offers three distinct advantages over the miR-E scaffold (46). First, the SIBR backbone may be intrinsically superior for multigene RNAi. Chung *et al.* previously demonstrated that chaining identical SIBR amiRNAs can enhance knockdown efficiency (11), and we additionally observed here that concatenating amiRNAs which targeted different genes was sufficient to increase knockdown potency. While this linkage-based enhancement has been seen for at least one other amiRNA backbone (9), effects of chaining miR-30-based amiRNAs are less consistent, and may even decrease amiRNA efficacy (40,80,81). Importantly, knockdown improvement due to concatenation was retained in eSIBR amiRNAs, in addition to the enhancement provided by the backbone modifications. Taken together, these results establish the eSIBR backbone as a promising tool for multi-gene knockdown. The second advantage of the eSIBR backbone is ease of cloning compared to the miR-E backbone, which requires de-novo synthesis of a 97-mer including the amiRNA target sequence and flanking optimized scaffold region (46). The eSIBR backbone can be easily swapped to replace existing wtSIBR scaffolds by restriction enzyme digestion and ligation as described in the original report (11). Furthermore, any previously designed SIBR amiRNAs can be inserted directly into the eSIBR backbone without the need to synthesize new sequences. Third, a recent breakthrough for functional zebrafish genetics used SIBR-based amiRNAs to create the first RNAi system to cause sufficient gene knockdown in this organism (82). In the study, SIBR/mi-155-based amiRNAs vastly outperformed amiRNAs expressed from the endogenous zebrafish miR-30 backbone, which posits that SIBR-based amiRNAs may be more potent in general than amiRNAs expressed from

the miR-30/E scaffolds. It will be of large interest to determine if the eSIBR backbone can further enhance knockdown in zebrafish as this may become an invaluable tool for an organism that currently has few methods for conditional loss-of-function studies.

We offer here an outline for efficient multi-gene knockdown, from amiRNA design through implementation using the eSIBR backbone. We showed the applicability of eSIBR-based miRNAs by potently knocking down three members of a gene family in cultured neurons using a lentiviral expression system, demonstrating the eSIBR backbone as a useful tool for RNAi-based research. We believe that the eSIBR backbone holds great promise for applications which may benefit from multi-target RNAi, such as tackling functional redundancy within gene families or even gene therapy-based methods requiring simultaneous knockdown of multiple genes.

SUPPLEMENTARY DATA

Supplementary Data are available at NAR Online.

ACKNOWLEDGEMENTS

We would like to thank Dr David Turner (University of Michigan) for providing the SIBR cassette, Dr Scott Stewart and Dr Kryn Stankunas (University of Oregon) for suggesting use of the SIBR system and providing their unpublished Gateway-compatible lentiviral destination vector and other lentiviral reagents and Dr Peter Scheiffele (University of Basel, Switzerland) for providing HA-Neuroligin and HA-Neurexin expression vectors.

FUNDING

National Institute of Neurological Disorders and Stroke [R01 NS065795 to P.W.]; Developmental Training Grant [NIH T32-HD07348 to D.K.F.]. Funding for open access charge: National Institutes of Health [P01 HD022486].
Conflict of interest statement. None declared.

REFERENCES

1. Fellmann,C. and Lowe,S.W. (2014) Stable RNA interference rules for silencing. *Nat. Cell Biol.*, **16**, 10–18.
2. Krol,J., Loedige,I. and Filipowicz,W. (2010) The widespread regulation of microRNA biogenesis, function and decay. *Nat. Rev. Genet.*, **11**, 597–610.
3. Ha,M. and Kim,V.N. (2014) Regulation of microRNA biogenesis. *Nat. Rev. Mol. Cell Biol.*, **15**, 509–524.
4. Filipowicz,W., Bhattacharyya,S.N. and Sonenberg,N. (2008) Mechanisms of post-transcriptional regulation by microRNAs: are the answers in sight? *Nat. Rev. Genet.*, **9**, 102–114.
5. Aagaard,L.A., Zhang,J., von Eije,K.J., Li,H., Saetrom,P., Amarzguioui,M. and Rossi,J.J. (2008) Engineering and optimization of the miR-106b cluster for ectopic expression of multiplexed anti-HIV RNAs. *Gene Ther.*, **15**, 1536–1549.
6. Yue,J., Sheng,Y., Ren,A. and Penmatsa,S. (2010) A miR-21 hairpin structure-based gene knockdown vector. *Biochem. Biophys. Res. Commun.*, **394**, 667–672.
7. Chang,K., Marran,K., Valentine,A. and Hannon,G.J. (2014) Generation of transgenic Drosophila expressing shRNAs in the miR-1 backbone. *Cold Spring Harb Protoc.***2014**, doi:10.1101/pdb.prot080762.
8. Yang,J.S., Maurin,T., Robine,N., Rasmussen,K.D., Jeffrey,K.L., Chandwani,R., Papapetrou,E.P., Sadelain,M., O'Carroll,D. and Lai,E.C. (2010) Conserved vertebrate mir-451 provides a platform for Dicer-independent, Ago2-mediated microRNA biogenesis. *Proc. Natl. Acad. Sci. U.S.A.*, **107**, 15163–15168.
9. Liu,Y.P., Haasnoot,J., ter Brake,O., Berkhout,B. and Konstantinova,P. (2008) Inhibition of HIV-1 by multiple siRNAs expressed from a single microRNA polycistron. *Nucleic Acids Res.*, **36**, 2811–2824.
10. Chen,S.C., Stern,P., Guo,Z. and Chen,J. (2011) Expression of multiple artificial microRNAs from a chicken miRNA126-based lentiviral vector. *PLoS One*, **6**, e22437.
11. Chung,K.H., Hart,C.C., Al-Bassam,S., Avery,A., Taylor,J., Patel,P.D., Vojtek,A.B. and Turner,D.L. (2006) Polycistronic RNA polymerase II expression vectors for RNA interference based on BIC/miR-155. *Nucleic Acids Res.*, **34**, e53.
12. Zeng,Y., Wagner,E.J. and Cullen,B.R. (2002) Both natural and designed micro RNAs can inhibit the expression of cognate mRNAs when expressed in human cells. *Mol. Cell*, **9**, 1327–1333.
13. Boudreau,R.L., Monteys,A.M. and Davidson,B.L. (2008) Minimizing variables among hairpin-based RNAi vectors reveals the potency of shRNAs. *RNA*, **14**, 1834–1844.
14. Silva,J.M., Li,M.Z., Chang,K., Ge,W., Golding,M.C., Rickles,R.J., Siolas,D., Hu,G., Paddison,P.J., Schlabach,M.R. *et al.* (2005) Second-generation shRNA libraries covering the mouse and human genomes. *Nat. Genet.*, **37**, 1281–1288.
15. Boden,D., Pusch,O., Silbermann,R., Lee,F., Tucker,L. and Ramratnam,B. (2004) Enhanced gene silencing of HIV-1 specific siRNA using microRNA designed hairpins. *Nucleic Acids Res.*, **32**, 1154–1158.
16. Lebbink,R.J., Lowe,M., Chan,T., Khine,H., Wang,X. and McManus,M.T. (2011) Polymerase II promoter strength determines efficacy of microRNA adapted shRNAs. *PLoS One*, **6**, e26213.
17. Grimm,D., Wang,L., Lee,J.S., Schurmann,N., Gu,S., Borner,K., Storm,T.A. and Kay,M.A. (2010) Argonaute proteins are key determinants of RNAi efficacy, toxicity, and persistence in the adult mouse liver. *J. Clin. Invest.*, **120**, 3106–3119.
18. Kanasty,R.L., Whitehead,K.A., Vegas,A.J. and Anderson,D.G. (2012) Action and reaction: the biological response to siRNA and its delivery vehicles. *Mol. Ther.*, **20**, 513–524.
19. Snove,O. Jr and Rossi,J.J. (2006) Toxicity in mice expressing short hairpin RNAs gives new insight into RNAi. *Genome Biol*, **7**, 231.
20. Grimm,D., Streetz,K.L., Jopling,C.L., Storm,T.A., Pandey,K., Davis,C.R., Marion,P., Salazar,F. and Kay,M.A. (2006) Fatality in mice due to oversaturation of cellular microRNA/short hairpin RNA pathways. *Nature*, **441**, 537–541.
21. Castanotto,D., Sakurai,K., Lingeman,R., Li,H., Shively,L., Aagaard,L., Soifer,H., Gatignol,A., Riggs,A. and Rossi,J.J. (2007) Combinatorial delivery of small interfering RNAs reduces RNAi efficacy by selective incorporation into RISC. *Nucleic Acids Res.*, **35**, 5154–5164.
22. Amendola,M., Passerini,L., Pucci,F., Gentner,B., Bacchetta,R. and Naldini,L. (2009) Regulated and multiple miRNA and siRNA delivery into primary cells by a lentiviral platform. *Mol. Ther.*, **17**, 1039–1052.
23. McBride,J.L., Boudreau,R.L., Harper,S.Q., Staber,P.D., Monteys,A.M., Martins,I., Gilmore,B.L., Burstein,H., Peluso,R.W., Polisky,B. *et al.* (2008) Artificial miRNAs mitigate shRNA-mediated toxicity in the brain: implications for the therapeutic development of RNAi. *Proc. Natl. Acad. Sci. U.S.A.*, **105**, 5868–5873.
24. Boudreau,R.L., Martins,I. and Davidson,B.L. (2009) Artificial microRNAs as siRNA shuttles: improved safety as compared to shRNAs in vitro and in vivo. *Mol. Ther.*, **17**, 169–175.
25. Giering,J.C., Grimm,D., Storm,T.A. and Kay,M.A. (2008) Expression of shRNA from a tissue-specific pol II promoter is an effective and safe RNAi therapeutic. *Mol. Ther.*, **16**, 1630–1636.
26. Myburgh,R., Cherpin,O., Schlaepfer,E., Rehrauer,H., Speck,R.F., Krause,K.H. and Salmon,P. (2014) Optimization of critical hairpin features allows miRNA-based gene knockdown upon single-copy transduction. *Mol. Ther. Nucleic Acids*, **3**, e207.
27. Wu,H., Ma,H., Ye,C., Ramirez,D., Chen,S., Montoya,J., Shankar,P., Wang,X.A. and Manjunath,N. (2011) Improved siRNA/shRNA functionality by mismatched duplex. *PLoS One*, **6**, e28580.

28. Judge,A.D., Bola,G., Lee,A.C. and MacLachlan,I. (2006) Design of noninflammatory synthetic siRNA mediating potent gene silencing in vivo. *Mol. Ther.*, **13**, 494–505.
29. Judge,A.D., Sood,V., Shaw,J.R., Fang,D., McClintock,K. and MacLachlan,I. (2005) Sequence-dependent stimulation of the mammalian innate immune response by synthetic siRNA. *Nat. Biotechnol.*, **23**, 457–462.
30. Cao,W., Hunter,R., Strnatka,D., McQueen,C.A. and Erickson,R.P. (2005) DNA constructs designed to produce short hairpin, interfering RNAs in transgenic mice sometimes show early lethality and an interferon response. *J. Appl. Genet.*, **46**, 217–225.
31. Alvarez,V.A., Ridenour,D.A. and Sabatini,B.L. (2006) Retraction of synapses and dendritic spines induced by off-target effects of RNA interference. *J. Neurosci.*, **26**, 7820–7825.
32. Bridge,A.J., Pebernard,S., Ducraux,A., Nicoulaz,A.L. and Iggo,R. (2003) Induction of an interferon response by RNAi vectors in mammalian cells. *Nat. Genet.*, **34**, 263–264.
33. Sledz,C.A., Holko,M., de Veer,M.J., Silverman,R.H. and Williams,B.R. (2003) Activation of the interferon system by short-interfering RNAs. *Nat. Cell Biol.*, **5**, 834–839.
34. Bauer,M., Kinkl,N., Meixner,A., Kremmer,E., Riemenschneider,M., Forstl,H., Gasser,T. and Ueffing,M. (2009) Prevention of interferon-stimulated gene expression using microRNA-designed hairpins. *Gene Ther.*, **16**, 142–147.
35. Nielsen,T.T., Marion,I., Hasholt,L. and Lundberg,C. (2009) Neuron-specific RNA interference using lentiviral vectors. *J. Gene Med.*, **11**, 559–569.
36. Shin,K.J., Wall,E.A., Zavzavadjian,J.R., Santat,L.A., Liu,J., Hwang,J.I., Rebres,R., Roach,T., Seaman,W., Simon,M.I. *et al.* (2006) A single lentiviral vector platform for microRNA-based conditional RNA interference and coordinated transgene expression. *Proc. Natl. Acad. Sci. U.S.A.*, **103**, 13759–13764.
37. Stegmeier,F., Hu,G., Rickles,R.J., Hannon,G.J. and Elledge,S.J. (2005) A lentiviral microRNA-based system for single-copy polymerase II-regulated RNA interference in mammalian cells. *Proc. Natl. Acad. Sci. U.S.A.*, **102**, 13212–13217.
38. Du,G., Yonekubo,J., Zeng,Y., Osisami,M. and Frohman,M.A. (2006) Design of expression vectors for RNA interference based on miRNAs and RNA splicing. *FEBS J.*, **273**, 5421–5427.
39. Hu,T., Fu,Q., Chen,P., Ma,L., Sin,O. and Guo,D. (2009) Construction of an artificial MicroRNA expression vector for simultaneous inhibition of multiple genes in mammalian cells. *Int. J. Mol. Sci.*, **10**, 2158–2168.
40. Sun,D., Melegari,M., Sridhar,S., Rogler,C.E. and Zhu,L. (2006) Multi-miRNA hairpin method that improves gene knockdown efficiency and provides linked multi-gene knockdown. *Biotechniques*, **41**, 59–63.
41. Barbaric,I., Miller,G. and Dear,T.N. (2007) Appearances can be deceiving: phenotypes of knockout mice. *Brief. Funct. Genomic. Proteomic.*, **6**, 91–103.
42. Grimm,D. and Kay,M.A. (2007) Combinatorial RNAi: a winning strategy for the race against evolving targets? *Mol. Ther.*, **15**, 878–888.
43. Herrera-Carrillo,E. and Berkhout,B. (2015) The impact of HIV-1 genetic diversity on the efficacy of a combinatorial RNAi-based gene therapy. *Gene Ther.*, **22**, 485–495.
44. Aagaard,L. and Rossi,J.J. (2007) RNAi therapeutics: principles, prospects and challenges. *Adv. Drug Deliv. Rev.*, **59**, 75–86.
45. Wang,S.L., Yao,H.H. and Qin,Z.H. (2009) Strategies for short hairpin RNA delivery in cancer gene therapy. *Expert Opin. Biol. Ther.*, **9**, 1357–1368.
46. Fellmann,C., Hoffmann,T., Sridhar,V., Hopfgartner,B., Muhar,M., Roth,M., Lai,D.Y., Barbosa,I.A., Kwon,J.S., Guan,Y. *et al.* (2013) An optimized microRNA backbone for effective single-copy RNAi. *Cell Rep.*, **5**, 1704–1713.
47. Auyeung,V.C., Ulitsky,I., McGeary,S.E. and Bartel,D.P. (2013) Beyond secondary structure: primary-sequence determinants license pri-miRNA hairpins for processing. *Cell*, **152**, 844–858.
48. Kwan,K.M., Fujimoto,E., Grabher,C., Mangum,B.D., Hardy,M.E., Campbell,D.S., Parant,J.M., Yost,H.J., Kanki,J.P. and Chien,C.B. (2007) The Tol2kit: a multisite gateway-based construction kit for Tol2 transposon transgenesis constructs. *Dev. Dyn.*, **236**, 3088–3099.
49. Hoy,J.L., Constable,J.R., Vicini,S., Fu,Z. and Washbourne,P. (2009) SynCAM1 recruits NMDA receptors via protein 4.1B. *Mol. Cell. Neurosci.*, **42**, 466–483.
50. Barrow,S.L., Constable,J.R., Clark,E., El-Sabeawy,F., McAllister,A.K. and Washbourne,P. (2009) Neuroligin1: a cell adhesion molecule that recruits PSD-95 and NMDA receptors by distinct mechanisms during synaptogenesis. *Neural Dev.*, **4**, 17.
51. Scheiffele,P., Fan,J., Choih,J., Fetter,R. and Serafini,T. (2000) Neuroligin expressed in nonneuronal cells triggers presynaptic development in contacting axons. *Cell*, **101**, 657–669.
52. Chih,B., Afridi,S.K., Clark,L. and Scheiffele,P. (2004) Disorder-associated mutations lead to functional inactivation of neuroligins. *Hum. Mol. Genet.*, **13**, 1471–1477.
53. Taniguchi,H., Gollan,L., Scholl,F.G., Mahadomrongkul,V., Dobler,E., Limthong,N., Peck,M., Aoki,C. and Scheiffele,P. (2007) Silencing of neuroligin function by postsynaptic neurexins. *J. Neurosci.*, **27**, 2815–2824.
54. Amarzguioui,M. and Prydz,H. (2004) An algorithm for selection of functional siRNA sequences. *Biochem. Biophys. Res. Commun.*, **316**, 1050–1058.
55. Fellmann,C., Zuber,J., McJunkin,K., Chang,K., Malone,C.D., Dickins,R.A., Xu,Q., Hengartner,M.O., Elledge,S.J., Hannon,G.J. *et al.* (2011) Functional identification of optimized RNAi triggers using a massively parallel sensor assay. *Mol. Cell*, **41**, 733–746.
56. Pei,Y. and Tuschl,T. (2006) On the art of identifying effective and specific siRNAs. *Nat. Methods*, **3**, 670–676.
57. Reynolds,A., Leake,D., Boese,Q., Scaringe,S., Marshall,W.S. and Khvorova,A. (2004) Rational siRNA design for RNA interference. *Nat. Biotechnol.*, **22**, 326–330.
58. Ui-Tei,K., Naito,Y., Takahashi,F., Haraguchi,T., Ohki-Hamazaki,H., Juni,A., Ueda,R. and Saigo,K. (2004) Guidelines for the selection of highly effective siRNA sequences for mammalian and chick RNA interference. *Nucleic Acids Res.*, **32**, 936–948.
59. Zuker,M. (2003) Mfold web server for nucleic acid folding and hybridization prediction. *Nucleic Acids Res.*, **31**, 3406–3415.
60. Darty,K., Denise,A. and Ponty,Y. (2009) VARNA: interactive drawing and editing of the RNA secondary structure. *Bioinformatics*, **25**, 1974–1975.
61. Morgan,M., Anders,S., Lawrence,M., Aboyoun,P., Pages,H. and Gentleman,R. (2009) ShortRead: a bioconductor package for input, quality assessment and exploration of high-throughput sequence data. *Bioinformatics*, **25**, 2607–2608.
62. Dull,T., Zufferey,R., Kelly,M., Mandel,R.J., Nguyen,M., Trono,D. and Naldini,L. (1998) A third-generation lentivirus vector with a conditional packaging system. *J. Virol.*, **72**, 8463–8471.
63. Brewer,G.J., Torricelli,J.R., Evege,E.K. and Price,P.J. (1993) Optimized survival of hippocampal neurons in B27-supplemented Neurobasal, a new serum-free medium combination. *J. Neurosci. Res.*, **35**, 567–576.
64. Khvorova,A., Reynolds,A. and Jayasena,S.D. (2003) Functional siRNAs and miRNAs exhibit strand bias. *Cell*, **115**, 209–216.
65. Schwarz,D.S., Hutvagner,G., Du,T., Xu,Z., Aronin,N. and Zamore,P.D. (2003) Asymmetry in the assembly of the RNAi enzyme complex. *Cell*, **115**, 199–208.
66. Fogel,A.I., Akins,M.R., Krupp,A.J., Stagi,M., Stein,V. and Biederer,T. (2007) SynCAMs organize synapses through heterophilic adhesion. *J. Neurosci.*, **27**, 12516–12530.
67. Shabalina,S.A., Spiridonov,A.N. and Ogurtsov,A.Y. (2006) Computational models with thermodynamic and composition features improve siRNA design. *BMC Bioinformatics*, **7**, 65.
68. Jagla,B., Aulner,N., Kelly,P.D., Song,D., Volchuk,A., Zatorski,A., Shum,D., Mayer,T., De Angelis,D.A., Ouerfelli,O. *et al.* (2005) Sequence characteristics of functional siRNAs. *RNA*, **11**, 864–872.
69. Matveeva,O.V., Nazipova,N.N., Ogurtsov,A.Y. and Shabalina,S.A. (2012) Optimized models for design of efficient miR30-based shRNAs. *Front. Genet.*, **3**, 163.
70. Chalk,A.M., Wahlestedt,C. and Sonnhammer,E.L. (2004) Improved and automated prediction of effective siRNA. *Biochem. Biophys. Res. Commun.*, **319**, 264–274.
71. Betancur,J.G., Yoda,M. and Tomari,Y. (2012) miRNA-like duplexes as RNAi triggers with improved specificity. *Front. Genet.*, **3**, 127.
72. Yoda,M., Kawamata,T., Paroo,Z., Ye,X., Iwasaki,S., Liu,Q. and Tomari,Y. (2010) ATP-dependent human RISC assembly pathways. *Nat. Struct. Mol. Biol.*, **17**, 17–23.
73. Okamura,K., Liu,N. and Lai,E.C. (2009) Distinct mechanisms for microRNA strand selection by Drosophila Argonautes. *Mol. Cell*, **36**, 431–444.

74. Noland,C.L. and Doudna,J.A. (2013) Multiple sensors ensure guide strand selection in human RNAi pathways. *RNA*, **19**, 639–648.
75. Patzel,V., Rutz,S., Dietrich,I., Koberle,C., Scheffold,A. and Kaufmann,S.H. (2005) Design of siRNAs producing unstructured guide-RNAs results in improved RNA interference efficiency. *Nat. Biotechnol.*, **23**, 1440–1444.
76. Tomari,Y., Du,T. and Zamore,P.D. (2007) Sorting of Drosophila small silencing RNAs. *Cell*, **130**, 299–308.
77. Forstemann,K., Horwich,M.D., Wee,L., Tomari,Y. and Zamore,P.D. (2007) Drosophila microRNAs are sorted into functionally distinct argonaute complexes after production by dicer-1. *Cell*, **130**, 287–297.
78. Mori,M., Triboulet,R., Mohseni,M., Schlegelmilch,K., Shrestha,K., Camargo,F.D. and Gregory,R.I. (2014) Hippo signaling regulates microprocessor and links cell-density-dependent miRNA biogenesis to cancer. *Cell*, **156**, 893–906.
79. Moy,R.H., Cole,B.S., Yasunaga,A., Gold,B., Shankarling,G., Varble,A., Molleston,J.M., tenOever,B.R., Lynch,K.W. and Cherry,S. (2014) Stem-loop recognition by DDX17 facilitates miRNA processing and antiviral defense. *Cell*, **158**, 764–777.
80. Zhou,H., Xia,X.G. and Xu,Z. (2005) An RNA polymerase II construct synthesizes short-hairpin RNA with a quantitative indicator and mediates highly efficient RNAi. *Nucleic Acids Res.*, **33**, e62.
81. Osorio,L., Gijsbers,R., Oliveras-Salva,M., Michiels,A., Debyser,Z., Van den Haute,C. and Baekelandt,V. (2014) Viral vectors expressing a single microRNA-based short-hairpin RNA result in potent gene silencing in vitro and in vivo. *J. Biotechnol.*, **169**, 71–81.
82. Giacomotto,J., Rinkwitz,S. and Becker,T.S. (2015) Effective heritable gene knockdown in zebrafish using synthetic microRNAs. *Nat. Commun.*, **6**, 7378.